AREA
WV
Lincoln

FRACTURE FLOW CAPACITY OF HYDRAULICALLY FRACTURED DEVONIAN SHALES

By

U. Ahmed
L. Buchholdt
A. S. Abou-Sayed

Submitted to

Columbia Gas System Services Corporation
1600 Dublin Road
Columbia, Ohio 53215

Attention: Eric Smith

Submitted by

Terra Tek, Inc.
University Research Park
420 Wakara Way
Salt Lake City, Utah 84108

TR 78-57
Sept 1978

ABSTRACT

Flow capacities were determined for induced fractures in cores taken from 3445 feet and 3695 feet in the Columbia Gas System Services Corporation Well #20403, located in Lincoln County, West Virginia. The samples from depth 3445 feet were from the 'Middle Brown Shale' and from depth 3695 feet the 'Lower Gray Shale,'. The work was aimed at assessing flow capacity damage potential of a number of water-based fracturing fluids. The fractures were propped with a partial monolayer (0.027 lb/ft^2) of 20/40 mesh sand.

At conditions simulating *in situ* closure stress (2700 psi) and temperature (70°F), the 'Middle Brown Shale' fracture flow capacity was reduced to 5 percent of the original flow capacity. For the 'Lower Gray Shale' (the *in situ* closure stress of 2900 psi, temperature 70°F) the reduced flow capacity was close to one percent of the original. In both shales the decrease in flow capacity resulted from sand embedment initiated by fracturing fluid softening of the rock as well as clay flocculation around the imbedded sand.

TABLE OF CONTENTS

	Page
Abstract	i
Table of Contents	ii
List of Figures	iii
List of Tables	iv
Introduction	1
Experimental Procedure	2
Discussion of Results	4
References	16
Appendix - Flow Capacity Measurements	17

LIST OF FIGURES

Figure	Description	Page
1	Trend of fracture flow capacity with the increase in effective pressure for 'Middle Brown Shale'	9
2	Trend of the effective fracture width with the increase in effective pressure for 'Middle Brown Shale'	10
3	Fracture face of the 'Middle Brown Shale' sample interacted by Waterfrac 20 W/CO_2	11
4	Trend of fracture flow capacity with the increase in effective pressure for 'Lower Gray Shale'	12
5	Trend of the effective fracture width with the increase in effective pressure for 'Lower Gray Shale'	13
6	Fracture face of the 'Lower Gray Shale' sample interacted by Waterfrac 20-40	14
7	Fracture face of the 'Lower Gray Shale' sample interacted by Superfoam	15
8	Schematic design of the flow set-up	19

LIST OF TABLES

Table	Description	Page
1	Fracturing Fluids	3
2	Test Conditions	3
3	Columbia Gas System Well #20403, Middle Brown Shale, 3445', Comparison of Fracture Flow Capacity	5
4	Columbia Gas System Well #20403, Middle Brown Shale, 3445', Comparison of Fracture Width	5
5	Columbia Gas System Well #20403, Lower Gray Shale, 3695', Comparison of Fracture Flow Capacity	7
6	Columbia Gas System Well #20403, Lower Gray Shale, 3695', Comparison of Fracture Width	7

INTRODUCTION

Degradation of matrix and fracture permeability due to the application of hydraulic fracturing fluid has been presented as one reason for the failure of massive hydraulic fractures (Davis, 1974; Clark, 1977). The selection of a fracturing fluid is not only dependent upon the fluids effectiveness in creating the fracture and transporting the proppants; it is also dependent on the degree of formation damage and plugging. In a recent study (Holditch, 1978) the overall productivity decrease in gas production from the combined effects of reservoir damage, relative permeability damage, capillary pressure damage and fracture conductivity damage were investigated. Reduction in fracture conductivity had significant effect on productivity. Thus, the necessity of experimentally determining the damaging effect of fracturing fluid to the flow capacity of the specific formation.

EXPERIMENTAL PROCEDURE

Core samples taken from Columbia Gas System Services Corporation Well #20403 at depths of 3445 feet and 3695 feet were used in this investigation. The samples for the 3445 feet depth were from the 'Middle Brown Shale' and 3695 feet depth from the 'Lower Gray Shale'. The work was aimed at assessing flow capacity damage of a number of water-based fracturing fluids to fractures propped with a partial monolayer of 20/40 mesh sand.

The core samples were saw cut and propped with a sand concentration of 0.027 lb/ft^2. Initially the cores were subjected to confining pressure of 90 psi for the proppants to settle in place. By flowing dry nitrogen gas through the propped channel, flow capacity measurements were taken. The change in flow capacity with effective pressure was determined by varying the confining pressure from 500 psi to 3500 psi; in all cases gas pressure within the fracture was maintained at 300 psi. Cantilevers were placed on the outer core surface to monitor changes in fracture width closure. Fracturing fluid was subsequently flowed through the propped fracture for four hours (to simulate field fracturing time) and the change in flow capacity with effective pressure was determined for the same confining pressure range.

The constituents of the fracturing fluids and the test conditions are presented in Table 1 and 2 respectively. All fracturing fluids were supplied by Dowell. Besides the fracturing fluids saturated nitrogen was flowed through the propped fracture to assess the fracture flow damage from water alone. After each sequence of tests the fractures were examined with an optical microscope to assess the degree of sand embedment, sand crushing, and clay flocculation in the fracture.

DISCUSSION OF RESULTS

Discussion of results are presented in light of the type of shales.

Middle Brown Shale: Figure 1 and Table 3 illustrate the change in the fracture flow capacity with increasing effective pressure for the virgin sample and after exposure to Waterfrac 20 W/CO_2 and saturated nitrogen. Figure 2 and Table 4 show the decreasing trend of the calculated effective fracture width with the increase in effective pressure for the same tests. The gentle slope of the curves for the virgin sample in both Figure 1 and 2 suggests that the fracture closed mainly as a result of proppant embedment. Figure 2 also includes a plot of the fracture width (derived from experimentally measuring the closure width) with effective pressure for the virgin sample and upon being interacted by Waterfrac 20 W/CO_2. This provides a qualitative and quantitative comparison between calculated and experimentally measured values.

Upon application of the fracturing fluid there is a marked reduction in fracture conductivity. Waterfrac 20 W/CO_2 fracturing fluid decreased the original flow capacity by approximately two orders of magnitude. Saturated nitrogen had an even greater effect on the flow capacity. This clearly explains the effect of water on the fracture surface.

Optical microscopic examination of the fracture face after interaction with Waterfrac 20 W/CO_2 is shown in Figure 4. Evidence of deep sand embedment is present with signs of clay flocculation around the proppants.

The following reasons can be accepted as causes for the overall decline in flow capacity due to fracturing fluid application:

TABLE 3

COLUMBIA GAS SYSTEM WELL #20403

MIDDLE BROWN SHALE

3445'

COMPARISON OF FRACTURE FLOW CAPACITY

Effective Pressure psi	Fracture Flow Capacity md-cm		
	Before Fracturing Fluid Flow	After Fracturing Fluid Flow	
		Waterfrac 20 W/CO_2	Saturated Nitrogen
200	92,000	2900	875
500	78,000	2550	850
1000	67,000	2150	810
2000	44,000	1880	760
3000	30,500	1670	730
3200	26,750	1650	720

TABLE 4

COLUMBIA GAS SYSTEM WELL #20403

MIDDLE BROWN SHALE

3445'

COMPARISON OF FRACTURE WIDTH

Effective Pressure psi	Fracture Width cm		
	Before Fracturing Fluid Flow	After Fracturing Fluid Flow	
		Waterfrac 20 W/CO_2	Saturated Nitrogen
500	.0220	.00720	.00440
1000	.0207	.00717	.00420
2000	.0190	.00690	.00392
3000	.0170	.00670	.00365
3200	.0155	.00668	.00360

1. The water in the water based fracturing fluids helped the fracture face to soften and result in sand proppant embedment.
2. From Figure 3 we have signs of material clusters only around the proppants and no damage to the surface where there were no proppants. This suggests the fracturing fluid has no chemical action; fracture surface damage beneath proppants indicates clay softening. There is no evidence of clay swelling.
3. Fracture flow capacity decrease is due to proppant embedment.

Lower Gray Shale: Figure 4 and Table 5 show the change in the fracture flow capacity with increasing effective pressure for the virgin sample and after exposure to Waterfrac 20-40, superfoam and saturated nitrogen. Figure 5 and Table 6 illustrate the decreasing trend of the calculated effective fracture width with the increase in effective pressure for the same tests. Similar to the 'Middle Brown Shale', Figure 4 and 5 suggest that the fracture of the virgin sample closed mainly as a result of sand proppant embedment. Figure 5 also includes a plot of the fracture width (derived from experimentally measuring the closure width) with effective pressure for the virgin sample and upon being interacted by Waterfrac 20-40.

Upon application of the fracturing fluid there is a marked reduction in fracture conductivity similar to that seen for the 'Middle Brown Shale'. Both the Waterfrac 20-40 and Superfoam decreased the virgin flow capacity by roughly three orders of magnitude. Waterfrac 20-40 causing slightly less damage than Superfoam. Saturated nitrogen decreased the virgin flow capacity between one and two orders of magnitude. This is less than the effect seen for 'Middle Brown Shale'. From two seperate studies, Leventhal (1978) and Mcketta (1978) it has been identified that 'Middle Brown Shale' has a higher

TABLE 5

COLUMBIA GAS SYSTEM WELL #20403

LOWER GRAY SHALE

3695'

COMPARISON OF FRACTURE FLOW CAPACITY

Effective Pressure psi	Fracture Flow Capacity md-cm			
	Before Fracturing Fluid Flow	After Fracturing Fluid Flow		
		Waterfrac 20-40	Saturated Nitrogen	Superfoam
200	88,000	380	3950	140
500	75,000	220	3600	105
1000	63,000	130	3200	77
2000	41,000	98	2475	52
3000	26,500	74	1910	35
3200	24,750	69	1800	33

TABLE 6

COLUMBIA GAS SYSTEM WELL #20403

LOWER GRAY SHALE

3695'

COMPARISON OF FRACTURE WIDTH

Effective Pressure psi	Fracture width cm		
	Before Fracturing Fluid Flow	After Fracturing Fluid Flow	
		Waterfrac 20-40	Superfoam
500	.0210	.0036	.00256
1000	.0205	.0026	.00227
2000	.01805	.00234	.00193
3000	.0160	.00210	.00165
3200	.0147	.00201	.00161

percentage of organic materials and calcium oxide (CaO). Organic material absorbs water and calcium oxide absorbs water by chemically reacting with water in the following manner:

$$CaO + 2H_2O \rightarrow 2Ca(OH)_2$$

This explains why the 'Middle Brown Shale' has a lower flow capacity than 'Lower Gray Shale' upon being interacted by saturated nitrogen.

Optical microscopic examination of the fracture face after interaction with Waterfrac 20-40 and Superfoam are shown in Figure 6 and 7 respectively. Evidence of deep sand proppant embedment is present with signs of clay flocculation around the proppants. Fracture face interacted by Superfoam has more flocculated clay.

Reasons for the reduction of flow capacity in the 'Lower Gray Shale' due to the interaction by the fracturing fluids are the same as for the 'Middle Brown Shale'.

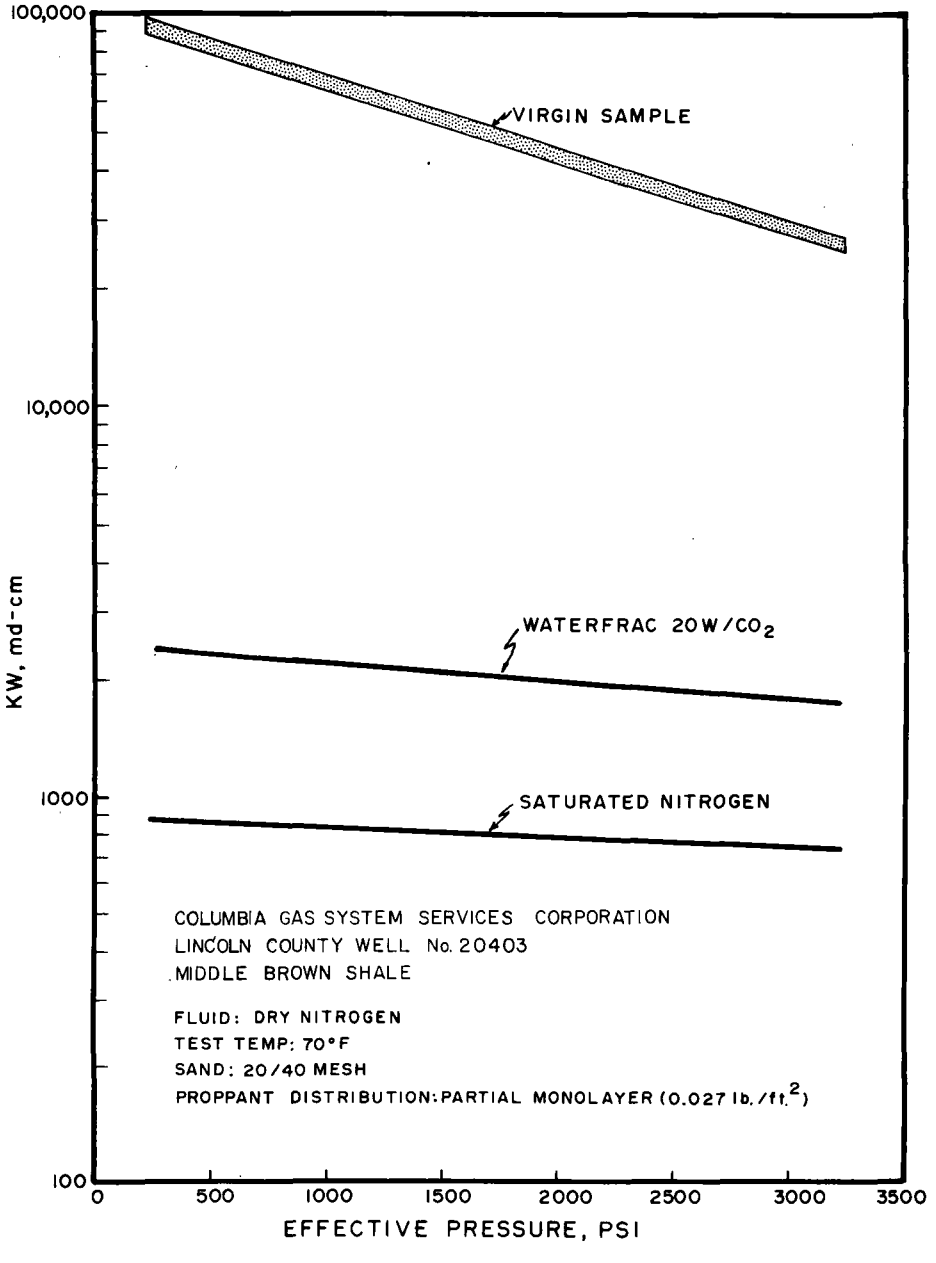

Figure 1. Trend of fracture flow capacity with the increase in effective pressure for 'Middle Brown Shale'.

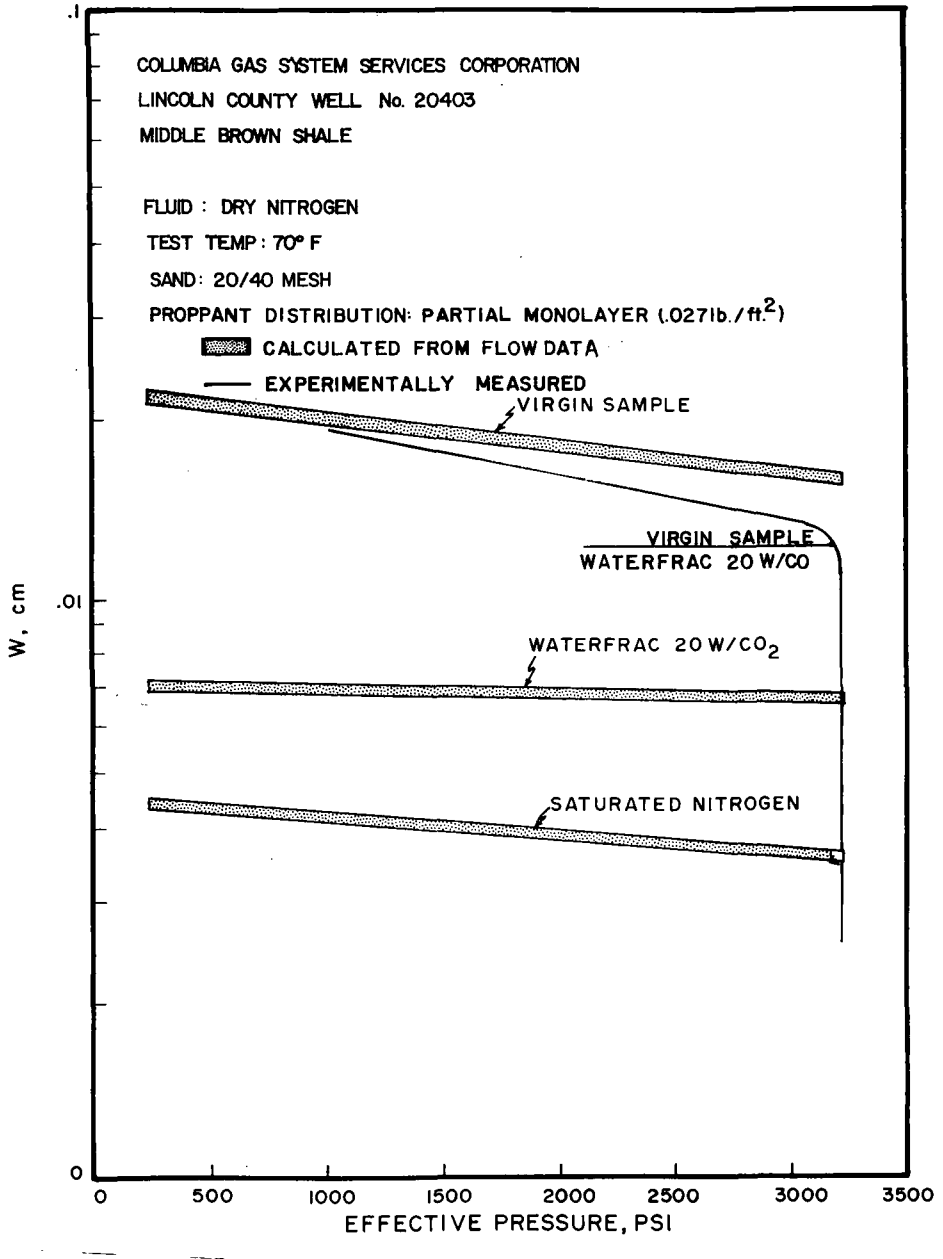

Figure 2. Trend of the effective fracture width with the increase in effective pressure for 'Middle Brown Shale'.

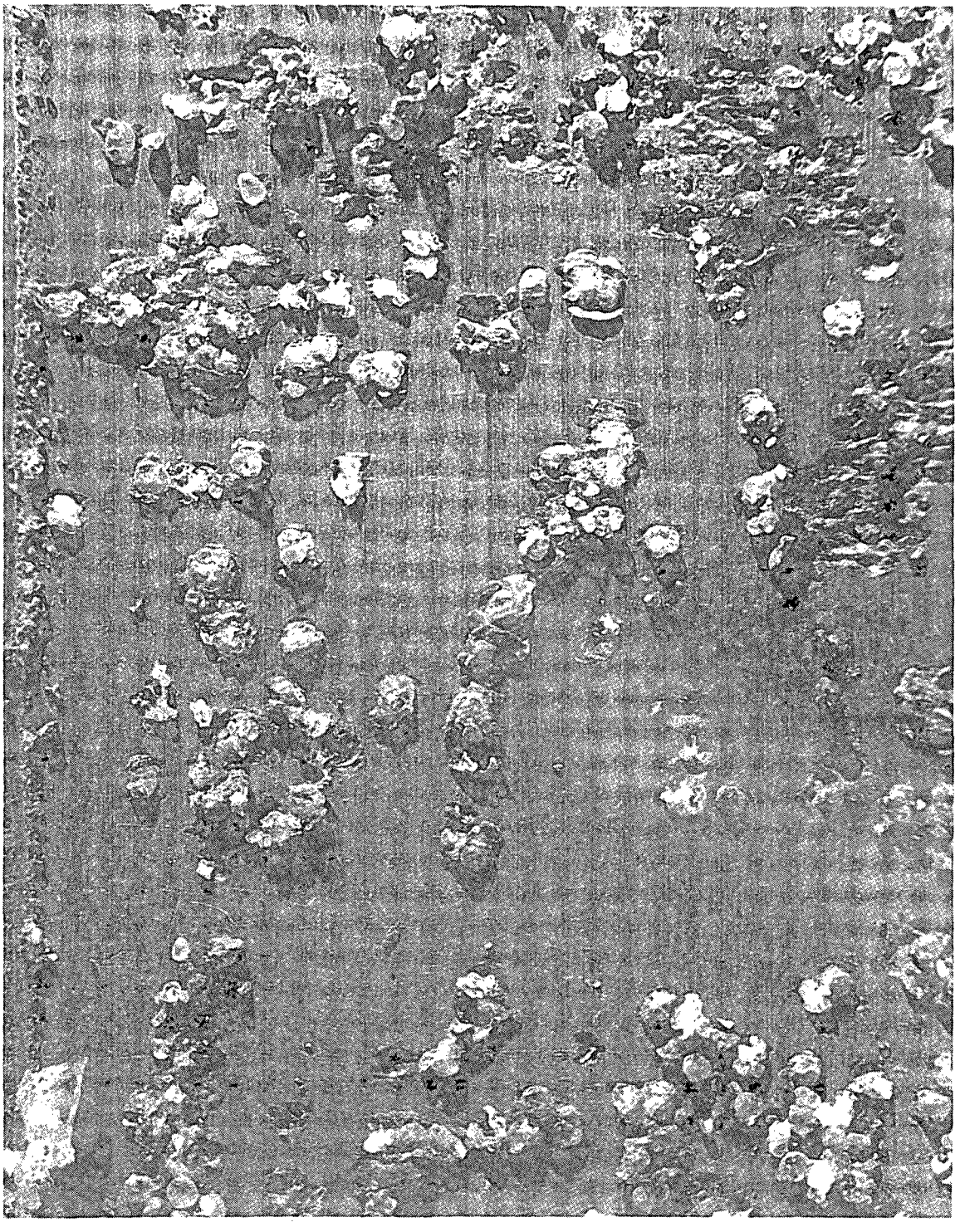

Figure 3. Fracture face of the 'Middle Brown Shale' sample interacted by Waterfrac 20 W/CO_2.

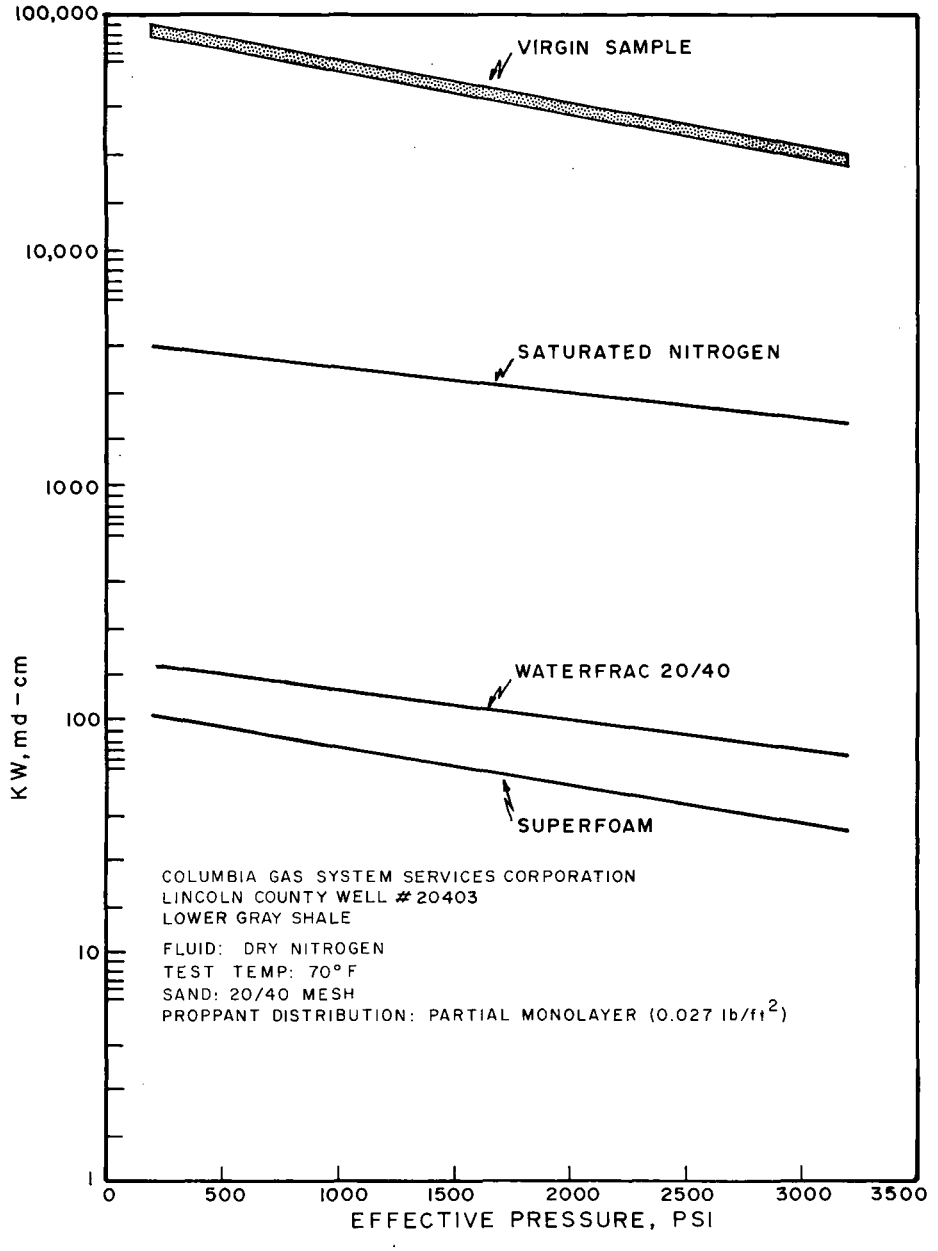

Figure 4. Trend of fracture flow capacity with the increase in effective pressure for 'Lower Gray Shale'.

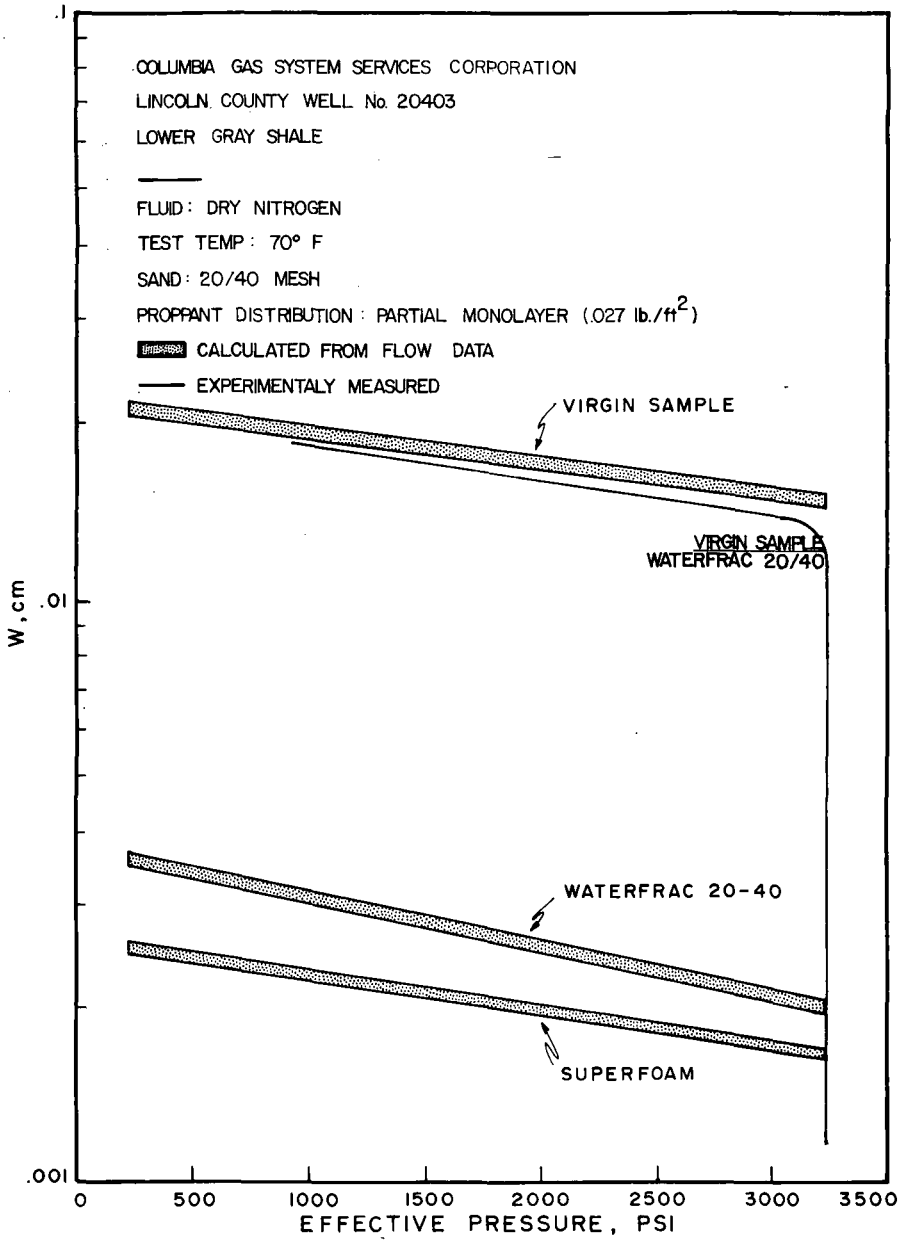

Figure 5. Trend of the effective fracture width with the increase in effective pressure for 'Lower Gray Shale'.

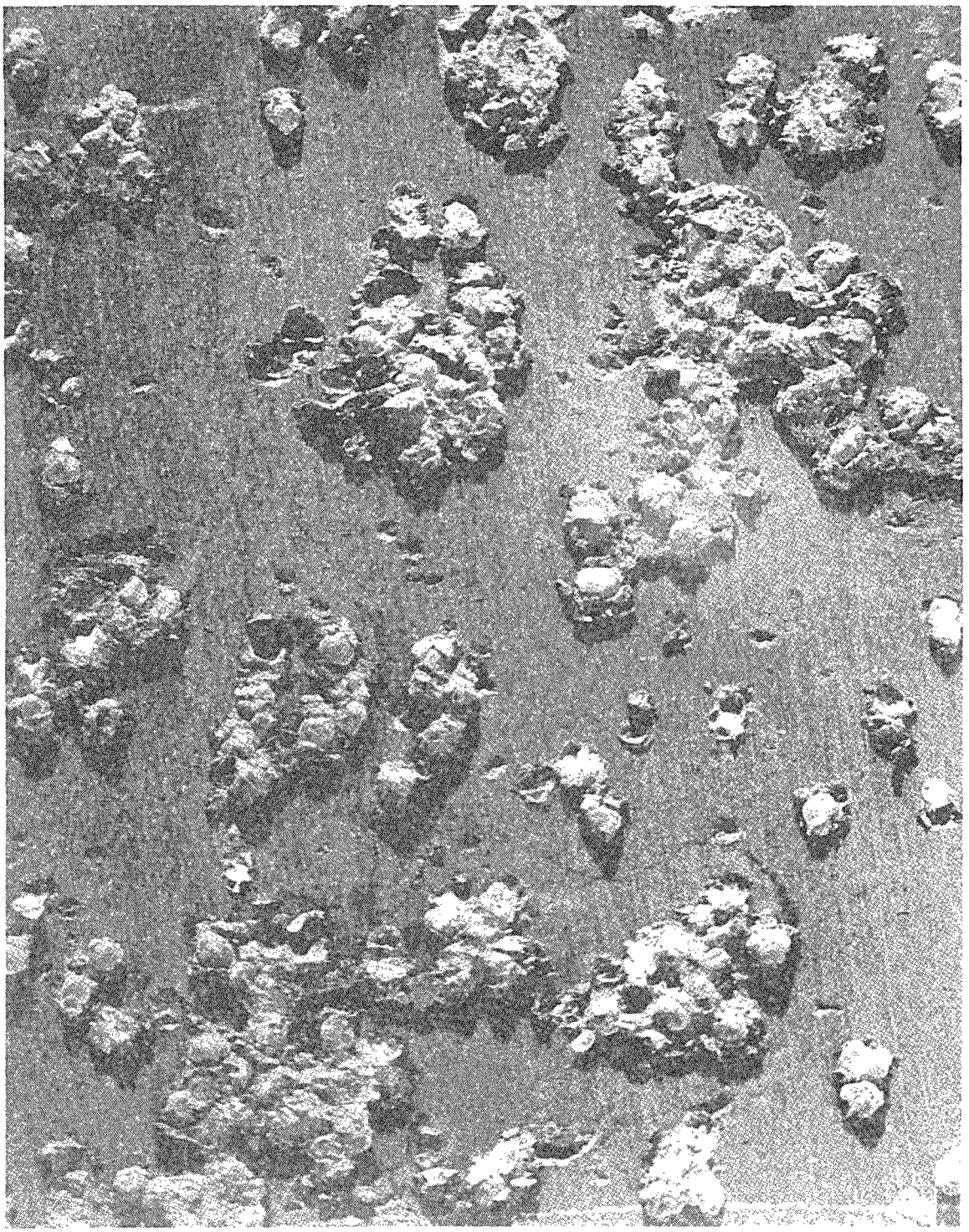

Figure 6. Fracture face of the 'Lower Gray Shale' sample interacted by Waterfrac 20-40.

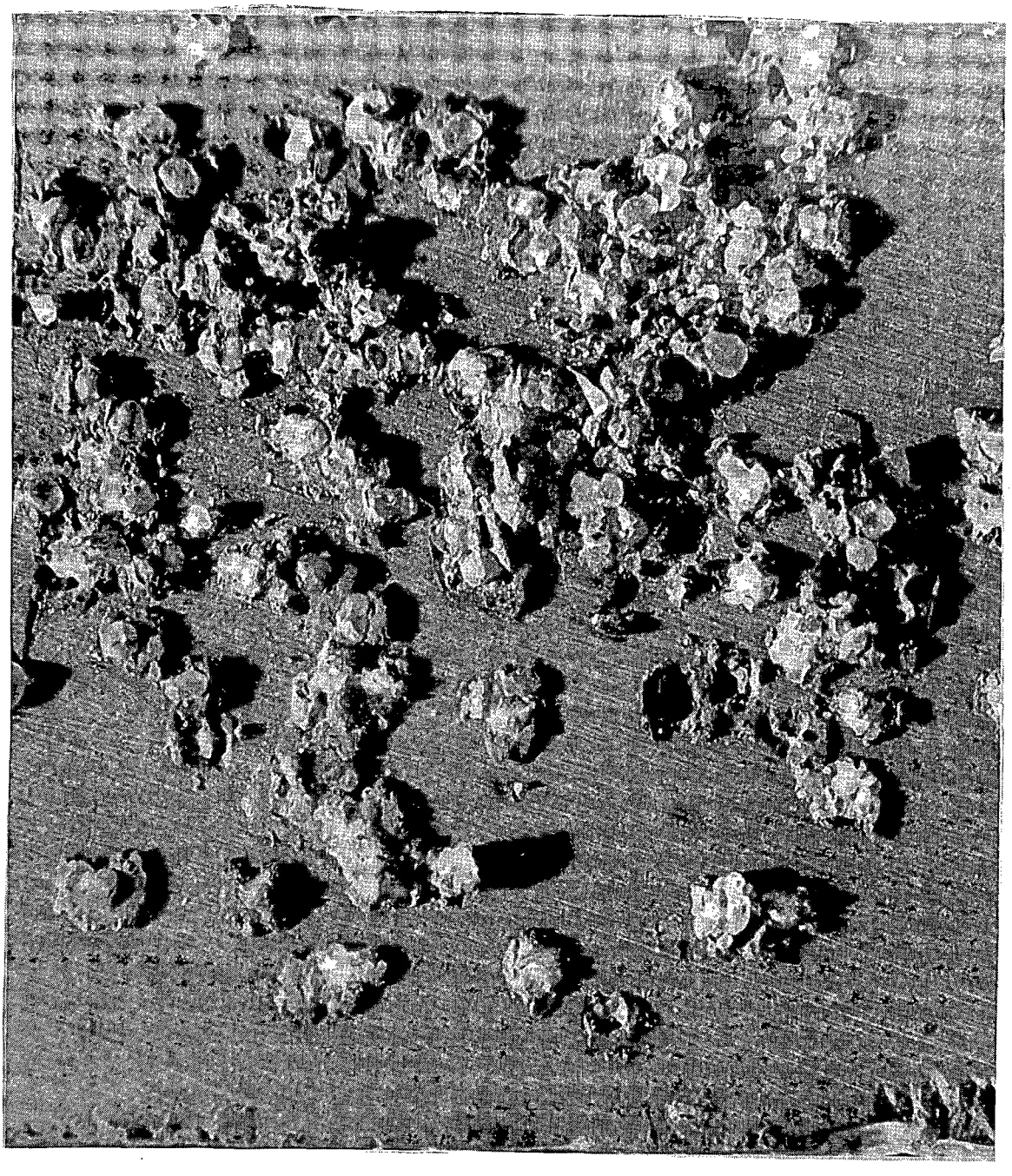

Figure 7. Fracture face of the 'Lower Gray Shale' sample interacted by Superfoam.

REFERENCES

Amyx, J. S., Bass, D. M., Jr., and Whiting, R. L., "Petroleum Reservoir Engineering - Physical Properties," McGraw Hill, Inc., pp. 70, (1960).

Clark, P. E., Harkin, M. W., Wahl, H. A., and Sievevert, J. A., "Design of a Large Vertical Prop Transport Model," 52nd Annual Fall Technical Conference and Exhibition of the SPE-AIME, Denver, Colorado, (October 9-12, 1977).

Craft, B. C., and Hawkins, M. F., "Applied Petroleum Reservoir Engineering," Prentice-Hall, Inc., Englewood Cliffs, N. J., pp. 882, (1959).

Davis, W. E., Jr., "Consideration for Fracture Stimulation of the Deep Morrow in the Anadarko Basin," SPE paper 5391 presented at Oklahoma City Regional Meeting, Oklahoma City, Oklahoma, (March 24-25, 1975).

Holditch, S. A., "Factors Affecting Water Blocking and Gas Flow from Hydraulically Fractured Gas Wells," SPE paper 7561 presented at the 53rd Annual Fall Technical Conference and Exhibition of the SPE-AIME, Houston, Texas, (October 1-3, 1978).

Leventhal, J. S., "Summary of Chemical Analyses and Some Geochemical Controls Related to Devonian Black Shales from Tennessee, West Virginia, Kentucky, Ohio, and New York," Proceedings from the Second Eastern Gas Shales Symposium, Volume 1, (October 1978).

McKetta, S. F., "Investigation of Hydraulic Fracturing Technology in the Devonian Shale," Proceedings from the Second Eastern Gas Shales Symposium, Volume 1, (October 1978).

APPENDIX

FLOW CAPACITY MEASUREMENTS

The flow capacity of a fracture (a product of fracture permeability and width of the fracture) is usually reported instead of the permeability because the fracture width is generally not known.

The calculation of the flow capacity of a fracture follows from a simple derivation of Darcy's law, presented by Amyx, *et al.*, (1960)

$$Q_o = \frac{1 \times 10^{-3}\ KA(P_i - P_o)}{\mu L} \qquad (1)$$

where,

Q_o = flow rate of outlet fluid (ml/sec)

K = permeability (millidarcy's)

A = cross-sectional area of flow (cm^2)

P_i = inlet pressure (atm absolute)

P_o = outlet pressure (atm absolute)

μ = viscosity of fluid (centipoises)

L = length of the sample (cm)

For a fracture the cross-sectional area (A) of flow is essentially:

$$A = W \times h \qquad (2)$$

where,

W = width of the fracture, cm

h = height of the fracture, cm.

Substitution of Equation (2) into (1) results in the following relationship or the flow capacity, KW, in md-cm.

$$KW = \frac{1x10^3\ L\mu Q_o}{h(P_i - P_o)} \qquad (3)$$

In the reported tests, nitrogen flowed in and out of the pressure vessel through small lines with resulting pressure losses; therefore, a second set of lines were used to sense gas pressures at the ends of the samples. In this way, and for steady state flow, pressures were measured directly and no corrections were needed for line losses. The gas flow rate was measured at atmospheric pressure at the end of small flow lines leading from the pressure vessel. The volumetric flow through the samples was determined by making the pressure correction between the flowmeter (at atmospheric pressure) and the sample mean pore pressure (assuming isothermal flow at 70°C). Figure 8 is a schematic diagram of the experimental set-up.

An estimate of the width of the flow channels in the unpropped fracture can be made assuming equivalent permeability for flow between parallel plates (Craft and Hawkin, 1959).

$$Q_o = \frac{W^2 A\ (P - P_o)}{1.74 \times 10^{-6} \mu L} \qquad (4)$$

Here again replacing the term A by Equation (2), we have:

$$W = \left\{ \frac{1.74 \times 10^{-6} \mu L\ Q_o}{h(P_i - P_o)} \right\}^{1/3} \qquad (5)$$

This same equation can be used to make an estimate of the *effective* width of the flow channels in propped fractures.

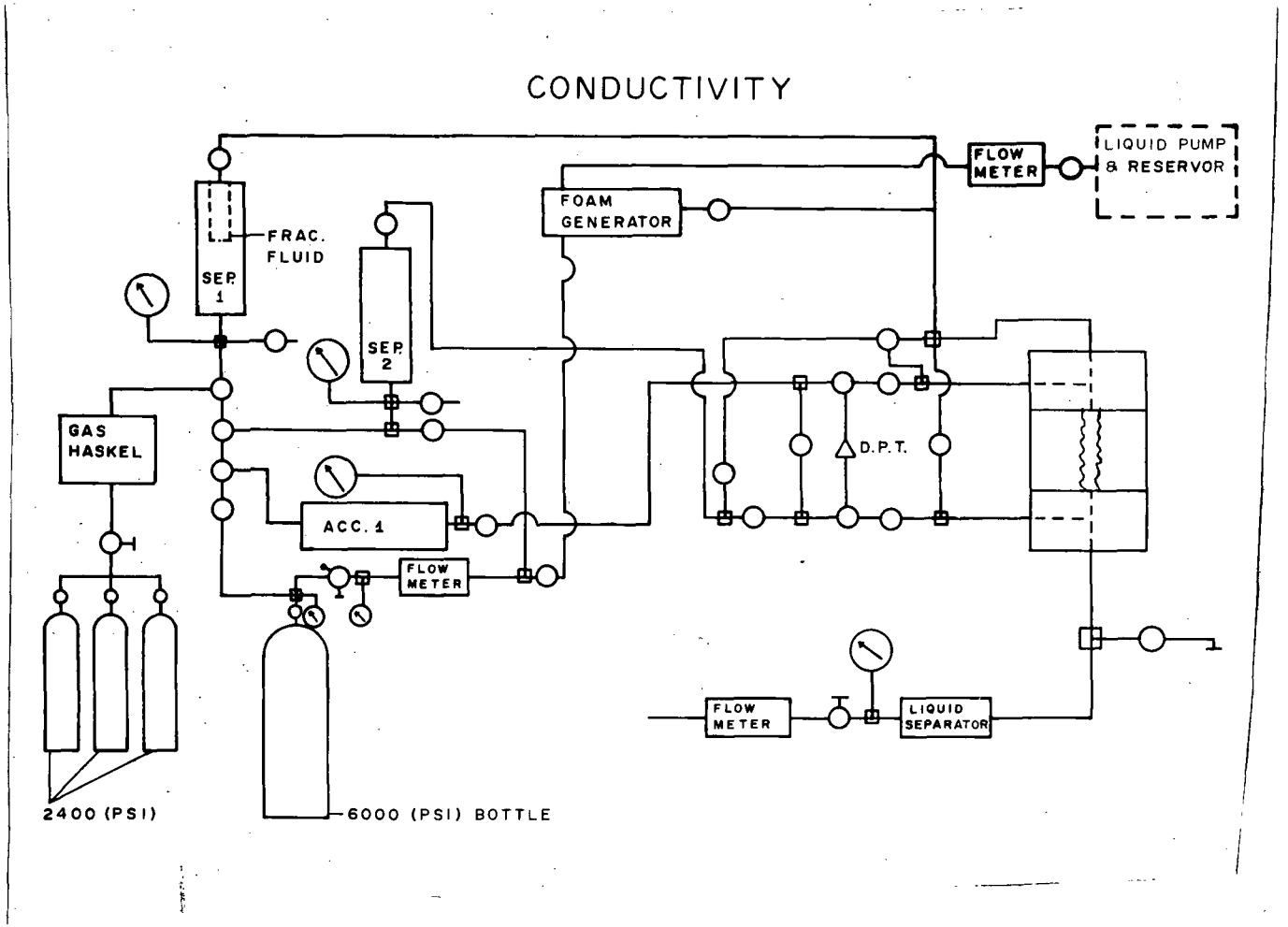

Figure 8. Schematic design of the flow set-up